

Understanding the effects of oriented susceptibility inclusions on the phase and magnitude of gradient echo signals

A. I. Blazejewska¹, S. Wharton¹, P. A. Gowland¹, and R. Bowtell¹

¹Sir Peter Mansfield Magnetic Resonance Centre, University of Nottingham, Nottingham, United Kingdom

Introduction Magnetic susceptibility differences generate inhomogeneities in the local magnetic field which modulate the magnitude and phase of the signals acquired in MRI. In the human body, static field perturbations can be caused by a number of materials including iron stores, red blood cells, myelin and contrast agents. Understanding the sensitivity of MR signals to the distribution of magnetic susceptibility is generally important for proper interpretation of T_2^* -contrast and of phase and susceptibility weighted images [1-3]. With the advent of susceptibility mapping [4] it has become particularly important to understand the relationship between microscopic structure in the distribution of susceptibility and the induced variation in the NMR frequency (and consequent phase accumulation), since it has recently been shown that in the presence of oriented, NMR-invisible susceptibility inclusions the measured phase may not be representative of the volume average magnetic susceptibility in a region [5]. To explore this behaviour, we therefore simulated the field perturbations generated in a uniform matrix containing ellipsoidal inclusions of different susceptibility and used this information to explore the effect of the shape of the inclusions on the phase and magnitude of the MR signal in the “static dephasing” regime [1].

Methods The magnetic field perturbation due to susceptibility variation was calculated using a Fourier-based method [6]. Simulations were run for inclusions consisting of ellipsoids of revolution with different aspect ratios ($q:1$) ranging from 6:1 = “needles” to 1:1 = spheres to 1:6 = “pancakes”. Three sizes of ellipsoid were included in each case, and the volume fraction (VF) of the inclusions was varied from 1-5 %. Non-overlapping inclusions were placed at random positions inside a larger cylindrical region, not crossing the external boundaries. Each ellipsoid’s axis of revolution was aligned with the applied magnetic field ($B_0 = 7T$) and a susceptibility difference, χ , between the inclusions and the matrix of 0.1 ppm was used, yielding values of $\alpha = \gamma\chi B_0$ of $187s^{-1}$. Fig. 1 shows a cross section through the structure in the cylindrical region and the resulting field perturbation. The complex MR signal from the whole region was calculated for TE values in the range of 1-100 ms, ignoring contributions from inside the ellipsoids. The variations of the phase and log of the signal magnitude with TE were fitted using polynomials in two different time ranges (0-25ms = short) and (75-100ms = long). The variation of the amplitudes of the resulting polynomial coefficients with the volume fraction and ellipsoid shape was then evaluated.

Results and Discussion We found that in all cases the natural log of the signal magnitude varied quadratically with TE ($\propto \text{const} + a_2 TE^2$) in the short echo time regime and linearly with TE ($\propto \text{const} + b_1 TE$) in the long echo time case. The phase was found to vary linearly with TE in both regimes, but with different constants of proportionality (written as c_1 and d_1 in the short and long TE regimes, respectively). The dominant polynomial coefficients were found to scale linearly with volume fraction. These findings are in agreement with theory previously described for spherical and cylindrical inclusions [1]. Importantly they indicate that the measured phase scales linearly with echo time and volume fraction even in the regime where the induced phase is $\gg 2\pi$ close to the inclusions. Example plots of the log of the magnitude and the phase of the signal (along with the polynomial fits in the two regimes) for spheres with a volume fraction of 3% and $\chi = 0.1\text{ppm}$ are shown in Fig. 2. Fig. 3 shows the variation of $c_1/(\alpha \times VF)$ with the demagnetising factor, D_{ze} , of the ellipsoids [7]. This linear variation of phase with D_{ze} in the short-TE regime was previously predicted from simple analysis of the average field in the matrix [8]. These data indicate that at short TE the measured phase depends strongly on the shape of the ellipsoids and that pancakes have a larger effect than needles. Fig. 4 shows the variation with the ellipsoid aspect ratio, q , of the other coefficients in appropriately-scaled, dimensionless forms ($a_2/(\alpha^2 \times VF)$, $b_1/(\alpha \times VF)$ and $d_1/(\alpha \times VF)$). The coefficient a_2 which characterises the variation of the signal magnitude at short TE, is largest when $q \sim 0.5$, indicating that slightly oblate ellipsoids oriented in the field direction have the strongest effect on signal decay in the short TE regime. This in contrast to the case of randomly oriented ellipsoids for which it has been shown that spheres ($q = 1$) cause the fastest signal decay [9]. Fig. 4 indicates that the coefficient, b_1 , which characterises the rate of exponential decay of the signal at long TE is approximately constant for intermediate q -values (0.33 to 2) taking a value of $\sim 0.4 \alpha VF$. This is the value predicted for a random arrangement of point dipoles with an equivalent volume average magnetic moment [1]. Similarly the coefficient, d_1 , which describes the effective angular frequency offset at long TE takes a value of $\sim 0.28 \alpha VF$ for intermediate q -values, again as predicted for point dipoles arranged in a cylindrical volume [1]. In this regime (TE=75-100 ms, intermediate q) the behaviour of the signal magnitude and phase is therefore largely independent of the shape of the ellipsoids and reflects the average susceptibility. This behaviour can be understood by considering the variation of the signal contributions with distance from the centre of each ellipsoid. Rapid phase variation around a prolate ellipsoid nulls the signal out to a radius that is approximately $\sqrt[3]{\alpha TE q^{-2} (2\pi)^{-1}}$, times the long dimension of the ellipsoid (for oblate ellipsoids q^{-2} is replaced with q). If this radius is larger than the extent of the ellipsoid then the region which generates a significant signal experiences only a dipolar field and so the behaviour can be adequately described using a distribution of dipoles. For the maximum value of $\alpha TE \sim 18.7$ considered here, this condition is satisfied for $0.34 < q < 1.7$. Additional simulations indicated that increasing αTE expands the range of q -values for which simple dipolar behaviour holds.

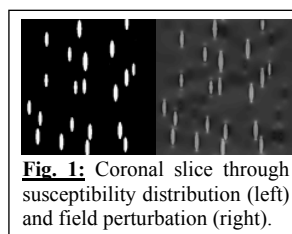


Fig. 1: Coronal slice through susceptibility distribution (left) and field perturbation (right).

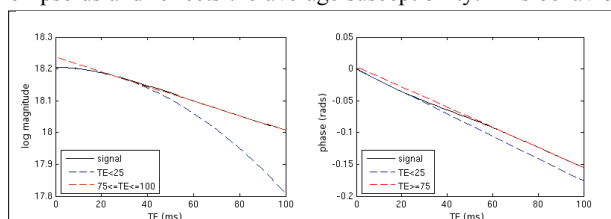


Fig. 2: Signal magnitude (left) and phase (right) variation with TE for spheres with VF=3%. Polynomial fits are shown for the two regimes.

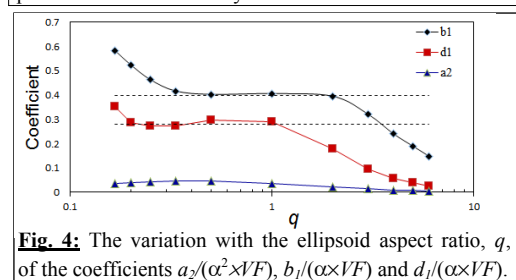


Fig. 4: The variation with the ellipsoid aspect ratio, q , of the coefficients $a_2/(\alpha^2 \times VF)$, $b_1/(\alpha \times VF)$ and $d_1/(\alpha \times VF)$.

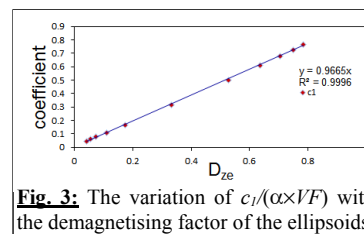


Fig. 3: The variation of $c_1/(\alpha \times VF)$ with the demagnetising factor of the ellipsoids.

Conclusions Numerical simulations of the MR signal in the presence of ellipsoidal inclusions have provided insight into the effect of the shape and concentration of oriented, high-susceptibility inclusions on the contrast in phase and T_2^* -weighted images. In future work, the effect of diffusion will be incorporated in the simulations.

References [1] Yablonskiy & Haacke, MRM, 1994, 32:749; [2] Duyn et al., PNAS, 2007,104:11796; [3] Haacke et al., MRM, 2004, 52:612; [4] Wharton & Bowtell, NIMG, 2010, 53:515; [5] He & Yablonskiy, PNAS, 2009, 106:13558; [6] Marques & Bowtell, Conc. in MR, 2005, 25(B):65; [7] Ulrich et al., JMR, 2003, 164; [8] Wharton & Bowtell, Proc ISMRM 2010; [9] Sukstanskii & Yablonskiy, JMR, 1001, 151:101.